Field Demonstration of a Cost-Optimized Solar Powered Electrodialysis Reversal Desalination System in Rural India

Wei He[a,b], Susan Amrose[a], Natasha C. Wright[a], Tonio Buonassisi[a], Ian M. Peters[a], Amos G. Winter, V[a]

[a]*Department of Mechanical Engineering, Massachusetts Institute of Technology, Cambridge, MA, United States*
[b]*School of Engineering, University of Warwick, Coventry, United Kingdom*

Abstract

This study provides experimental validation of a previously published optimal design theory for photovoltaic (PV)-powered electrodialysis reversal (EDR) desalination systems. The prior work describes the co-optimization of PV and EDR subsystems, and flexible operation to accommodate daily and annual solar irradiance variability, significantly reducing water cost. This study presents the fabrication of a PV-EDR pilot system designed using the co-optimization theory and field testing results from the rural village of Chelluru, India. Testing in the field enabled observation and evaluation of real-world factors on system performance, resulting in updates to the previous theory to include unaccounted factors that affect costs, including: filling and draining of water tanks, salt and water accumulation in tanks from prior batches, unexpected energy losses due to locally purchased converters, and scaling in the ED stack. Therefore, water cost in the PV-EDR pilot system was updated from previous estimates based on field performance. The estimated capital cost and lifetime cost of the Chelluru system are 34% and 45% lower, respectively, than the corresponding costs if the PV-EDR system was designed using conventional design practice. The theory and experimental insights presented in this paper will enable desalination engineers to better design and optimize PV-EDR systems.

Keywords: Cost-optimized, Electrodialysis Reversal, Field-Test, Photovoltaic

1. Introduction

India is experiencing the worst water crisis in its history [1], with one billion people living under severe water scarcity at least one month of the year [2]. The Indian government projects that the country's demand for water will be twice the available supply by 2030 [1]. Brackish groundwater with total dissolved solids (TDS) more than 500 mg/L underlies 60% of the land in India [3]. These levels are above the Bureau of Indian Standards for Drinking Water recommendation [4]. Almost 73% of Indian villages use groundwater as their primary drinking water source [5].

Currently, reverse osmosis (RO) is widely used in villages across India to desalinate brackish groundwater, powered primarily by grid electricity [6]. These systems are commercially maintained through the sale of drinking water at ₹2-3 per 12 L ($\approx$ 2.4-3.6 USD/m^3) [7, 8]. However, rural electrification is incomplete and unreliable. In rural areas with access to grid electricity, only 7% of households with electricity report no power outages, 18% report outages of up to four hours a day, and 20% experience intermittent power supply throughout most of the day [9]. The poor quality and intermittence of grid power results in either less water produced or oversizing on-grid RO plants to ensure a satisfactory amount of product water, which increases water cost.

Solar photovoltaic (PV)-powered brackish water desalination has recently emerged as an alternative for India due to the challenges of grid reliability, the abundance of solar energy, decreasing costs of PV panels, and an increasing awareness of environmental sustainability [10]. The performance and economic cost of a PV-powered desalination system significantly depend on feed water composition, geographic location, and system capacity. Because of the power system's capital cost, off-grid desalination systems cost much more than current on-grid systems; for village-scale RO plants commonly used

in India, the cost of the PV power system is more than the cost of the RO system itself [8]. A previous investigation [8] of solar PV-powered brackish water solutions informed by industry, manufacturers, non-governmental organizations, government agencies, and end users concluded that there are several benefits of electrodialysis (ED) over currently installed RO systems for rural India. Compared to RO, ED has lower energy consumption per unit of water produced (75% less at desalinating 1000 mg/L and 30% less at desalinating 3000 mg/L), greater recovery ratio (nearly double that of current village RO systems), longer membrane lifetime (2-3 times longer), and lower sensitivity to chlorine and feed water changes. These factors could contribute to smaller power system size, less groundwater wastage, lower membrane maintenance and replacement cost, and better adaptability with a broader range of feed water salinities, likely to result in a lower water cost in India.

The technical performance and energy consumption of PV-powered electrodialysis reversal (PV-EDR) desalination has been investigated previously in lab-scale and pilot-scale systems. Ortiz et al. [11] developed a PV-ED model and validated its ability by prototyping a lab-scale batch EDR brackish water desalination system without battery storage in a lab-scale batch system. Gonzalez et al. recently conducted a lab-scale investigation of a PV-ED batch system that desalinated brackish water from TDS 5,500 mg/L to 300mg/L with a specific energy consumption (SEC) of ED desalination of 5.46 kWh/m^3 [12]. In 1987, Adiga et al. built a pilot-scale 1 m^3/day PV-powered continuous ED system in the Thar Desert capable of desalinating 5,000 mg/L to 1,000 mg/L with an SEC of approximately 4 kWh/m^3 [13]. In the same year, Kuroda et al. [14] designed and constructed a pilot-scale batch mode PV-ED seawater desalination system in Nagasaki, Japan, producing 2-5 m^3 of drinking water at a TDS of 400 mg/L per day. This system was designed to align ED power consumption flexibly to the power supplied by the solar PV system by splitting its operation into two modes: 1) a high-power mode to partially desalinate the feed water at mid-day, and 2) a low-power mode to desalinate the partially-desalinated water to freshwater in the morning and afternoon.

These pilot-scale experiments were conducted over thirty years ago. Over the last three decades, PV power systems have become much more prevalent and their costs have substantially decreased. The market conditions of solar PV and desalination significantly alter the optimal PV-EDR system required to achieve the highest performance at the lowest capital and operating cost. In addition, due to solar intermittence and water consumption variations, only a combined understanding of PV generation and ED desalination processes will enable the creation of a holistic model capable of exploiting synergies between solar energy intermittence, drinking water demand variation, and location-dependent water composition to design a cost-optimized system.

An optimized PV-EDR system design should achieve a suitable production rate, low capital cost, and low lifetime cost. This depends on a series of complex interdependent trade-offs between elements, such as capital cost versus operational cost, pumping power versus ED process power, etc. Conventional design practices optimize subsystems sequentially - in this case, the EDR subsystem (defined as the EDR stack including membranes and electrodes, pumps, and water tanks) is specified to produce a certain production rate, followed by the PV subsystem (defined as the PV panels, batteries, and inverter) designed to provide the required power to meet the production requirement. These methods can be effective, but can result in oversized (and unnecessarily costly) systems that have to produce a given amount of water even on cloudy days. Conventional design practice may ignore the coupling effects between subsystems, for example minimizing the ED stack to reduce cost, while increasing battery capacity to run for more hours. They may also miss opportunities for flexible operation, where daily water production could vary in sync with available solar irradiance, provided on average production meets consumption demands.

As an alternative approach, Bian et al. proposed a co-optimal system design theory that individually considers the PV and EDR subsystems in a holistic model [15], allowing these subsystems to be cost- and performance-optimized simultaneously by considering flexible operation. A PV-EDR system designed for a rural Indian village and co-optimized using the theory was able to achieve a 42% reduction from the USD40,138 capital cost of the PV-EDR system designed using conventional practice [15]. To achieve this significant cost reduction, the co-optimal system design theory in [15] combines various strategies that have been used individually in the literature, including optimizing system design parameters (e.g. solar PV area, number of

pumps, membrane areas, etc.) [16, 17, 18, 19, 20], investigating system structure [21, 22], and utilizing effective optimization algorithms [23]. Another key to the cost reduction in this study by the co-optimization is flexible water production at the operational level that accommodates daily changes in solar irradiance, with overproduction on sunny days and water buffer storage tanks for long-term energy storage [15]. These cost minimization strategies of using water tanks as a surrogate energy storage to maximize solar utilization and minimize battery cost are similar to the modelling work on a solar-powered RO system for a relatively similar system size [24], and integrated desalination systems with pumped hydro energy storage used in much large system size [25, 26, 27]. However, none of these prior works provided experimental validation of the reported performance or costs.

Therefore, given our past work in [15] was theoretical, the present study aims to make this theory relevant to real-world conditions and useful for other desalination researchers and commercial engineers. Importantly, compared to most prior studies that use simulation tools to investigate system designs and minimize water cost [16, 17, 18, 19, 20, 24, 25, 26, 27], in this study we evaluated the real-world effects on the theoretically optimized designs by building and testing a community-scale, 6 m^3/day PV-EDR experimental prototype in the rural village of Chelluru, India. This study elucidates pain points not captured in prior work, describes updated co-optimization theory to address them and accurately reflect real-world factors, and presents experimental results that substantiate the accuracy of the theory as well as the cost savings that can be attained through PV-EDR co-optimization.

2. The co-optimization of the PV and EDR subsystems

The behavior of the PV and EDR subsystems are coupled reciprocally such that components in each subsystem closely interact with each other to realize the clean energy to clean water conversion. A PV-EDR system design using conventional engineering practice – which follows a serial process of specifying a daily production volume and operation time, ED stack size, and power subsystem size – is described in Appendix A. This design approach does not consider either the two-direction coupling between the PV subsystem and the EDR subsystem, or the component-level interactions between the two subsystems. Alternatively, the co-optimal design theory defines a PV-EDR system as an intermixed set of components involved in the conversion of solar energy to clean drinking water. The PV subsystem includes the PV panels, inverter, and batteries. The EDR subsystem includes the ED stack, pumps, DC power supply, and water storage tanks. The coupled model is summarized here; full details can be found in [15, 28, 29].

The energy flow between the solar PV panels, the batteries, and the ED stack is determined by the battery's state of charge and the water level in the water storage tank (Fig. 1). Depending on the operations, the power and energy flows in the PV-EDR system include,

$$\begin{aligned}
&\text{Charging:}\\
&P_{ED} = (P_{pv} - P_{batt,charge})\eta_{inv}\\
&E^t_{batt} = E^{t-1}_{batt} + \delta t(P_{pv} - P_{ED}/\eta_{inv})\eta_{batt}\\
&P_{batt,charge} = \frac{E^t_{batt} - E^{t-1}_{batt}}{\delta t}, \text{and}\\
&\text{Discharging:}\\
&P_{ED} = (P_{pv} + P_{batt,discharge})\eta_{inv}\\
&E^t_{batt} = E^{t-1}_{batt} - \delta t(P_{ED}/\eta_{inv} - P_{pv})\\
&P_{batt,discharge} = \frac{E^{t-1}_{batt} - E^t_{batt}}{\delta t},
\end{aligned} \tag{1}$$

where E_{batt} is energy stored in batteries, η_{inv} is the efficiency of inverter, P_{pv} is solar PV power, and η_{batt} is battery efficiency, which associates with both charging and discharging batteries. The superscript t denotes a specific time step. The power consumption of the ED desalination system, P_{ED}, is

$$P_{ED} = P_{desal} + P_{pump}. \tag{2}$$

Integrating the power with time, the SEC of an ED batch is

$$SEC_{ED} = \frac{(E_{desal} + E_{pump})}{V_p}, \tag{3}$$

where E_{desal} and E_{pumps} are energy consumption due to the applied voltage and pumping, respectively, V_p is the volume of the water production per batch (i.e. the batch size), and P_{pump} is the pumping power. P_{desal} is the power consumption for desalinating water, which is

$$P_{desal} = \frac{V_{total} I}{\eta_{DC}}, \tag{4}$$

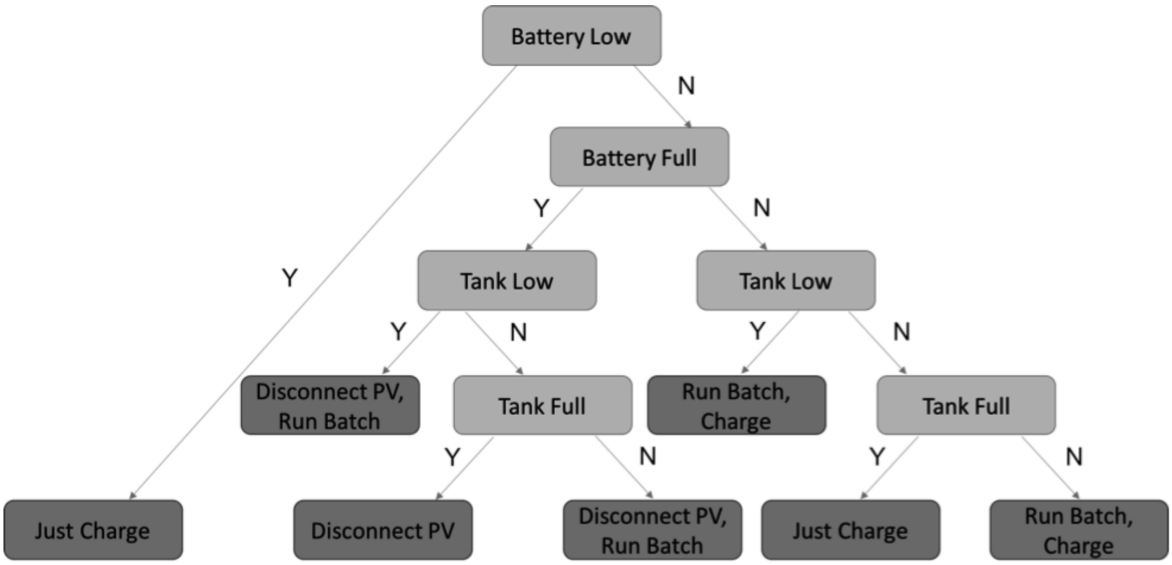

Figure 1: Logic tree for the power system module, detailing the conditions for charging the batteries and running an EDR batch [15].

where η_{DC} is the efficiency of the DC supply that applies a voltage to the electrodes, V_{total} is the voltage applied to the electrodes, and I is the current through the membranes. The ED stack is modeled as an analogous DC circuit with the voltage applied at the electrodes. Considering voltage drops over various components, the equivalent DC circuit model voltage is

$$\begin{aligned} V_{total} &= V_{el} + NV_{mem,y} \\ &+ Ni_y[(R^b_{d,y} + R^b_{c,y} + \\ &+ R^{BL}_y + R^{AEM} + R^{CEM})], \end{aligned} \tag{5}$$

where N is the number of cell pairs in the stack, i_y is the per-segment current density, and $R^b_{a_y}$, $R^b_{c_y}$, R^{BL}_y, R^{AEM}, and R^{CEM} are the area resistance associated with the bulk diluate and concentration streams, the concentration boundary layers, and the membranes, respectively. V_{el} and $V_{mem,y}$ are the potential across the electrodes and each membrane pair, respectively.

The total instantaneous current is the sum of all current densities multiplied by the flow channel segment length (L/Y, Y is the number of segments in the channel considered for simulation), width (W), and the open-area porosity of the turbulence promoting channel spacer (ϕ_A),

$$I = \phi_A(\frac{WL}{Y})\sum_{y=1}^{Y} i_y. \tag{6}$$

As indicated by Eq. 5 and Eq. 6, the power consumption of ED desalination depends on the varying concentration of both the diluate and concentration streams during the desalination process. In the holistic model, the rates of change of the concentration in the diluate and concentrate tanks are modelled as

$$\frac{dC^b_{d,0}}{dt} = \frac{Q_d}{V^{tank}_d}[C^b_{d,outlet} - C^b_{d,inlet}], \text{and} \tag{7}$$

$$\frac{dC^b_{c,0}}{dt} = \frac{Q_c}{V^{tank}_c}[C^b_{c,outlet} - C^b_{c,inlet}]. \tag{8}$$

The rates of change of the concentration of the diluate and concentrate steams inside of the ED

stack are

$$\frac{dC^b_{d,y}}{dt} = \frac{1}{NV^{cell}_y}[Q_d(C^b_{d,y-1} - C^b_{d,y}) - \frac{N\phi I_y}{zF} + \frac{NA_yD^{AEM}(C^{AEM}_{c,y} - C^{AEM}_{d,y})}{l^{AEM}} + \frac{NA_yD^{AEM}(C^{CEM}_{c,y} - C^{CEM}_{d,y})}{l^{CEM}}], \text{and} \quad (9)$$

$$\frac{dC^b_{c,y}}{dt} = \frac{1}{NV^{cell}_y}[Q_c(C^b_{c,y-1} - C^b_{c,y}) + \frac{N\phi I_y}{zF} - \frac{NA_yD^{AEM}(C^{AEM}_{c,y} - C^{AEM}_{d,y})}{l^{AEM}} - \frac{NA_yD^{AEM}(C^{CEM}_{c,y} - C^{CEM}_{d,y})}{l^{CEM}}], \quad (10)$$

where C is the concentration, Q is the flow rate, z is the ion charge, F is Faraday constant, and N is the number of cell pairs.

The co-optimized design of the Chelluru system was undertaken using our PV-EDR holistic model to design the ED stack, select the pumps, and size the PV panels and the batteries [15]. The model takes the feed water salinity, desired output water salinity, and desired averaged daily water production as fixed inputs, the number of cell pairs, applied stack voltage, and batch size as the design variables, and simulates the ED desalination process. This can be done for every day within a year of solar irradiance data for a given location. The system is optimized by randomly changing the design variables using a particle swarm optimization algorithm and predicting capital cost and water production reliability. The mass transfer and pumping in the ED desalination subsystem dictate the power consumption of the ED subsystem. By coupling this power consumption with the solar power available and battery storage, the PV-EDR model connects the EDR and solar power subsystems and enables their co-optimization simultaneously. Full details of the optimization process can be found in [15].

3. PV-EDR system in Chelluru, India

3.1. Chelluru village in rural India

Chelluru is a village near Hyderabad, India having a population of more than 2,000 people and groundwater salinity of 1,300-1,500 mg/L, varying with the seasons. The current local drinking water demands are primarily met by an on-grid RO system, which has been maintained by Tata Projects Ltd. for more than eight years. The solar irradiance and temperature data of the region of Chelluru were obtained from the National Solar Radiation Database SUNY database [30]. Global Horizontal Irradiance (GHI) was used for the solar power system design.

3.2. System configuration in the village

The prototype PV-EDR system optimized for Chelluru is shown in Fig. 2, and its specifications are listed in Table 1. Table 2 lists the parameters of the Chelluru pilot system that were used to simulate the prototype's performance. Of particular note, the locally purchased AC to DC converter efficiency was lower than that used in prior system simulations in [15], and lower than typical values of 80-90%. The poor performance of the converter was likely due to the fact that two converters had to be wired in series to produce the required voltage applied to the ED stack, and they were locally manufactured with questionable quality. Alternative manufacturers will be investigated for the deployment of future, commercial systems.

Table 1: System design of the PV-EDR pilot.

Design Variables	**value**
PV area [m^2]	40
Battery capacity [kWh]	16
Water storage volume [m^3]	10
ED cell pairs	56
Batch size [m^3]	0.45

The PV-EDR prototype was designed to meet 100% demand at all times given variations in solar irradiance, with the least system capital cost

Table 2: Energy conversion efficiencies used for simulating the pilot PV-EDR desalination system. The DC supply efficiency was measured. The inverter efficiency was from its datasheet. Battery efficiency from [15] was used for simulating the system.

Parameters	**Value**
Inverter efficiency	88%
DC power supply efficiency	52 ± 2%
Battery efficiency	90%

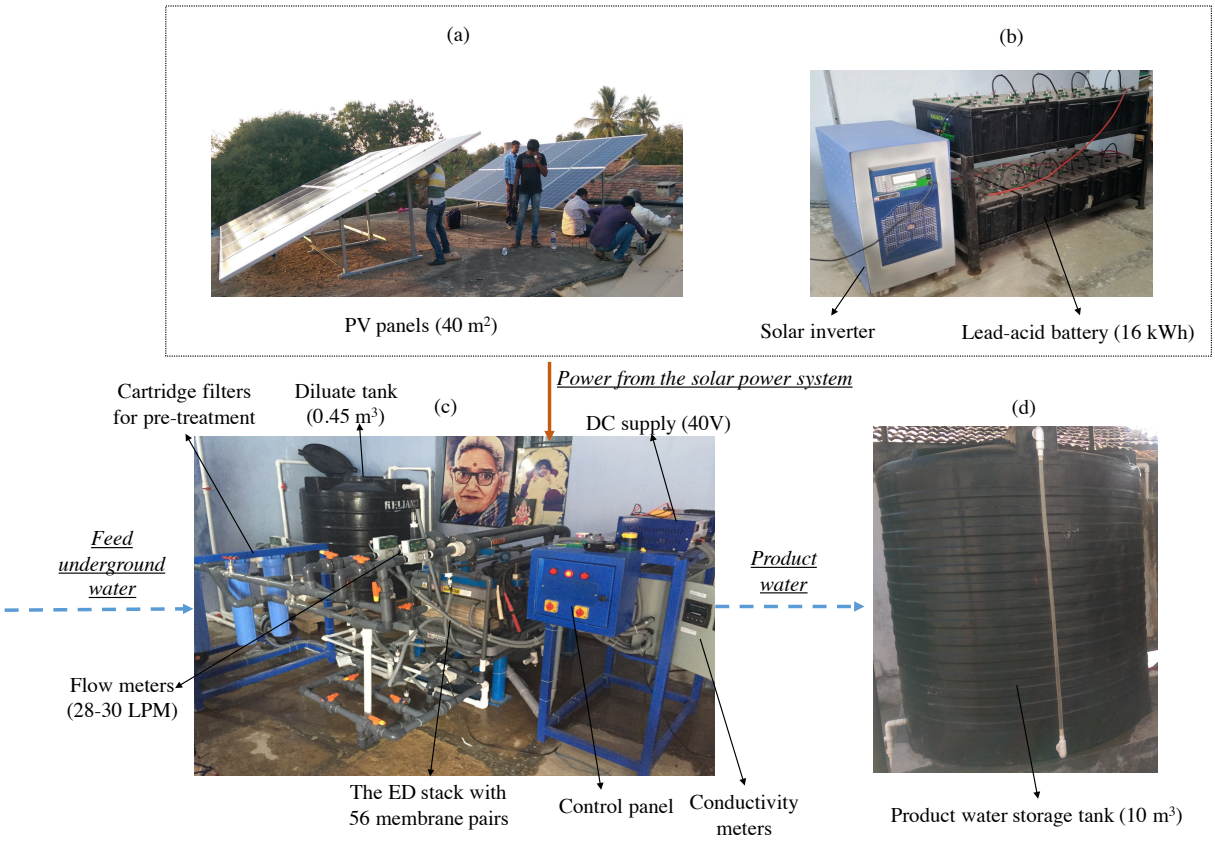

Figure 2: The system built in Chelluru India. (a) The installed rooftop solar panels. (b) The installed inverter and battery storage. (c) The installed ED system. (d) The installed water storage. The solid line indicates power flow. The dashed line indicates water flow.

using off-the-shelf components and batch EDR operation. The prototype was first installed in Chelluru in 2017, and was initially designed using the results from [15]. As in the original study, the system operated in a batch configuration, where water was recirculated through the ED stack from a diluate and concentrate tank as long as necessary to achieve the desired product salinity. The original design was for a 10 m^3 per day system, which did not consider the energy and time requirements for filling and draining tanks before and after desalination in an ED batch. However, the time used for filling and draining in the Chelluru system was almost 1/3 of the desalination time (as shown in Section 4), which limits the operating hours and the volume of water production per day in the village. As a result, the Chelluru pilot PV-EDR system presented herein produced 6 m^3 per day in practice. Nevertheless, the volume of water production is sufficient for Chelluru according to the recommended water intake minimum in the range of 2.5-3.0 liters per day per capita [31], and the measured water consumption in the village (Fig. 6).

Two changes were made to the model in [15] to improve the performance prediction of the actual tested PV-EDR system in Chelluru. First, the model in [15] assumed the same initial concentration of both the diluate and brine streams (feed concentration). However in practice, it is difficult to completely drain the brine and diluate tanks when a batch is finished due to the finite height of the outlet above the bottom of the tank. Additionally, some water remains in the ED stack. Both factors result in a starting batch concentration that is different between the two flows. A correction factor, $C_c^0 = 1.5C_d^0$, was used in the present simulation to reflect the concentration difference between the diluate and concentrate streams at the beginning of the batch. The second major change to the simulation was the addition of time in a batch to fill and

drain the tanks.

The system was originally designed to be operated with a recovery of >80%. However, during the first several weeks of initial tests in Chelluru, significant salt precipitation was observed within the ED stack and brine tank. Performance results during this period can be found in [6]. The scaling propensity is dependent on the groundwater composition. The composition of Chelluru feed water was measured in [29] and is reported in Table 5 in Appendix C. The feed water in Chelluru was particularly high in calcium with a pH of 7.02 ± 0.12. These conditions made the Chelluru site particularly susceptible to scaling of calcium carbonate.

To prevent or mitigate scaling, several approaches were applied to the pilot system, including: 1) reduction of the recovery ratio from 80% to 60%, which reduced the maximum brine concentration during desalination; 2) development of an acid rinsing procedure to regularly dissolve and flush out precipitated salts, if any; and 3) pH adjustment to pH <6 by manually adding small quantities of acid to the concentrate tank. Manual acid dosing was performed in which the pH of the brine was reduced from 7 (± 0.03) to 5.4-6 (± 0.03) before each batch in most batches. To do this, a pH 0.68-0.71 solution of HCl and diluate from a previous batch was added in appropriate amounts, 2 - 4 L (± 1%), during recirculation until the pH reading stabilized to a value below 6.0. With these adjustments, the salt precipitation was significantly mitigated, enabling field testing of the pilot PV-EDR system. The reduced water recovery ratio was a temporary solution to facilitate prolonged data collection; a return to >80% recovery is expected in the future. It should be noted that this recovery ratio is still higher than that of the onsite on-grid RO system maintained by Tata Projects Ltd., which is 30-40%. Also, the 60% recovery ratio did not diminish the purpose of this study, which was to assess and demonstrate the pilot system performance and cost in the field, and validate the co-optimization theory used to design it.

All components except the ED stack were purchased in India by the project partner Tata Projects Ltd. The model of the ED stack is AQ3-1-2-50-35 that is manufactured by Suez Water Technology, with the parameters listed in Table 1. Electrodes of the ED stack are made of titanium. The ion exchange membranes are manufactured by SUEZ, which are homogeneous ion exchange films cast in sheet form on reinforcing synthetic acrylic cloth fabrics. The model numbers of the CEM and AEM membranes are CR67HMR and AR204SZRA, respectively. Detailed information of these membranes and materials can be found in [32]. To configure this stack (which normally has two electrical stages) into a single electrical stage stack, the first electrical stage was not electrified. This ED stack was used because it was readily available, and enabled the pilot system field testing in Chelluru with relatively low investment and short lead time. In the future, a single-stage ED stack would be used, and thus, the cost of one pair of electrodes was considered in this study.

Grundfos CM 3-3 pumps of stainless steel SS316 were selected for the system to prevent corrosion. Ten 12 V, 135 Ah lead-acid batteries, equating to a 16.2 kWh lead-acid battery bank, were installed for electrical energy storage considering a minimum state of charge of 50%, indicating that the minimum capacity of energy stored in the battery bank is half of the batteries' original full capacity. A UTL solar power inverter was selected for the system, which is an integrated unit and consists of a solar charger with maximum power point tracking, and an inverter that connects the PV panels, batteries, and ED system. The UTL inverter monitored and recorded voltage (± 3%) and current (± 3%) of the batteries and solar cells, as well as the voltage and current of the AC output to the ED system, in which a locally purchased rectifier converted AC to DC to power the electrodes.

The Chelluru system has two Omega FP1406 flow meters (± 0.2LPM) and four Omega PX309 (± 2%) pressure gauges in order to monitor the flow rates in the diluate and concentrate channels at the entry and pressure drop though the ED stack. To measure conductivity of the diluate and concentration streams, connectivity instruments CDCE-90 in-line conductivity probes (± 2%) and CDCN-91 conductivity controllers were utilized. All flow and conductivity sensors are interfaced with National Instruments NI9203 data acquisition modules for measurement data logging. The flow rate of 5.5 LPM, and the flow rates of 28-30 LPM (correspoindg to a >6 cm/s linear velocity in both cases) were held in the electrode rinse streams and both the diluate and concentrate channels, respectively. Because of the batch size and water recovery of 60%, the diluate tank and brine tank were selected to be 500 L and 1,000 L, respectively. Labels of water levels were made in both tanks to measure appropriate volumes such that the diluate volume was 0.45 m^3

(± 4%), and the brine volume was 0.30 m^3 (± 7%). The pump power in the pilot was about 390 W (± 4%) per pump according to the AC/DC inverter power data recorded.

A constant voltage, 40 V± 2 V, was applied at the electrodes of the ED stack. This voltage was selected such that the limiting current density was not exceeded at the end of a desalination batch. The pilot system was manually operated. At the end of each batch, the polarity of the applied voltage was reversed and eight total valves at the entrance and exit of the stack were used to switch the diluate and concentrate channels in the stack. The reversal operation is for reducing the scaling propensity in ED desalination [33]. The village water consumption of the adjacent RO plant was monitored using a HOBO data logger that was attached to the solenoid valve used to dispense water in 12 L allotments to paying customers.

4. Results and discussion

4.1. Single-batch performance

In this section, a single-batch operation, one of 13 total batches on 02 May 2018, is used to validate the ED model. (Note that all batches resulted in similar performance, as indicated in Fig. 4 in Section 5.2). Simulation predictions are within 9% of the pilot test measurements. In Fig. 3(a), the initial TDS of the brine is ∼600 mg/L higher than the initial TDS of the diluate due to the small volume of high concentration brine that remained in the piping, the stack flow channels, and tanks from the previous batch. This difference was accounted for in the simulation as discussed in Section 3.2. As shown in Fig. 3(b), the simulated current is higher than the measured current at the beginning of the batch. The higher current in simulation is caused by the build-up of the diffusion boundary layers in the channels. The simulation initializes with homogeneous concentration fields in both flow channels. When the simulation starts, concentration polarization quickly builds up in the boundary layers, rapidly increasing the resistances of the solutions in the boundaries and causing a large drop in the current profile in a very short time. This rapid change was not resolved by the current measurement. The total power profile (desalination plus pumping) is plotted in Fig. 3(c), with two pumps running to recirculate the concentrate and diluate streams. The power consumed by the AC/DC converter is proportional to the current because the ED batch was operated at a constant applied voltage.

Table 3: Energetic performance from single ED batch, including both simulation and experimental results. The energetic performance and desalination rate calculated are based on a product concentration of 300 mg/L.

System energetic performance	**Value**
Modeled SEC, [kWh/m^3]	1.79
Experimental SEC, [kWh/m^3]	1.68 ± 0.13
Modeled desalination rate, [m^3/h]	0.80
Experimental desalination rate, [m^3/h]	0.85 ± 0.04

Table 3 compares the SEC and desalination rate for a single-batch operation in which the diluate was desalinated from 1,350 mg/L TDS to 300 mg/L TDS. The simulated SEC has an error 6.6% of the experimental measurement, and the simulated desalination rate has an error of 6.0% of the experimental measurement. The SEC prediction is consistent with the measurement within estimated uncertainty, and the desalination rate is within 1.25 standard deviations, being slightly faster in the pilot test than the model predicted. A reason contributing to this discrepancy is the concentration-conductance conversion in the model, which assumes the feed is sodium chloride. The groundwater is actually a mixture of multiple ions (as listed in Appendix C), so higher conductance in both the concentrate and diluate speed up the desalination compared to the rate of desalinating sodium chloride. In addition, other factors related to measurements, such as measuring conductivity of the diluate tank at a single point at the inlet of the ED stack, which then determines the timing of the end of the batch, may contribute to the discrepancy. Using this single point value to determine the end of the batch assumes the diluate tank is well-mixed with negligible conductivity change in the pipes. The inaccuracy of the conductivity reading due to the volumetric mixing may lead to an additional error of the desalination rate, which is not considered in the current analysis. In the future, a multiple-point measurement or an enhanced mixing protocol could be implemented to improve this measurement. As it stands, the ED model predicts the energetic performance of desalinating brackish water in Chelluru well, validating a foundational compo-

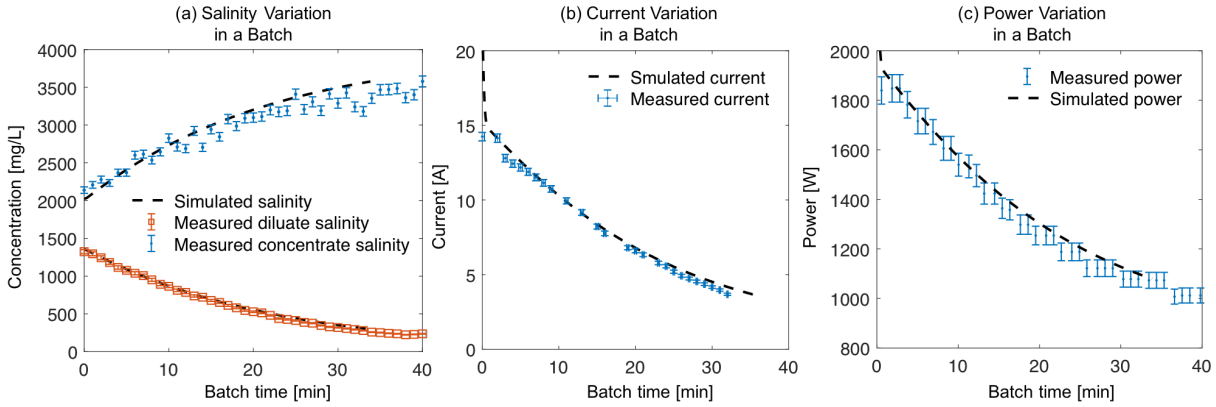

Figure 3: Field testing and modeling results of a single ED batch. The concentration profiles, current profile, and power consumption profile are plotted in (a), (b), and (c), respectively. A conversion factor of 0.6 is considered to convert conductivity to concentration in Fig. 3(a). The error bars of the concentration profiles, current profile, and power profile are ±2%, ±1%, and ±3%, respectively.

nent of the PV-EDR holistic model. The measured SEC of the single-batch operation is much less than the reported SEC of the pilot-scale PV-EDR system [12, 13, 14], due to the much less concentrated feed water.

4.2. Single-day performance

Figure 4 shows the performance of the PV-EDR pilot on a day of operation (here, data from May 2, 2018 are used). Fig. 4(a) demonstrates 13 ED batches were achieved on that day, and produced 6 m^3 of potable water. From Fig. 4(a), the operation time was slightly longer in the pilot than in the simulation. This is mainly due the time required to adjust the pH immediately after filling the tanks ($\leq$15 min per batch), which was initiated to mitigate scaling encountered during the first few months of testing. During pH adjustment, two pumps were running to recirculate and mix both tanks, which can be seen in the measured ED power profile in Fig. 4(b) and Fig. 4(a). The energy consumption due to acid dosing was very small ($\leq$ 2% of the total ED SEC as shown in Fig. 6), and the temporary manual acid dosing procedure is likely to be improved. Therefore, at this stage, the pumping power and time required for pH adjustment were not considered in the simulation.

From Fig. 4(a), the daily battery cycle of the PV-EDR system is observed. The initial energy capacity of the battery was taken as a reference set to 0 kWh. When desalination started at 7 AM, the battery was discharged to power the first batch before the sun was fully up. With the increase of solar power, the energy stored in the battery started to increase until the battery was fully charged at mid-day. The battery started to discharge again at 5:30 pm when the PV power became insufficient. The battery bank was large enough to power the system over the entire day.

Figure 5 breaks down the solar energy utilization in terms of SEC in kWh per m^3 of potable water produced. As indicated by the Sankey diagram, approximately 46% of the solar energy was not specifically used for any purpose on this particular day, but it contributed to an energy buffer necessary to overcome seasonal and unexpected solar variations on monthly and yearly timescales (discussed in the next section). Fifty-four percent of the solar energy was utilized for producing water and charging the batteries during the day. Of this 54%, 85% of the utilized solar energy was used to desalinate brackish water via two methods: 1) solar direct drive, or solar energy directly powering the ED process without batteries; and 2) battery-assisted drive in which batteries with or without solar energy powered the ED process when solar power was not sufficient or available. On this day, the batteries were charged more than they were discharged, and 2% of the solar energy was stored in the batteries for future water production. Thirteen percent of the solar energy was lost due to inefficiencies in the inverter and batteries.

The adjacent RO plant at the Chelluru site allowed us to measure the village water consumption by monitoring the water distributed. The net water production of the PV-EDR prototype and water

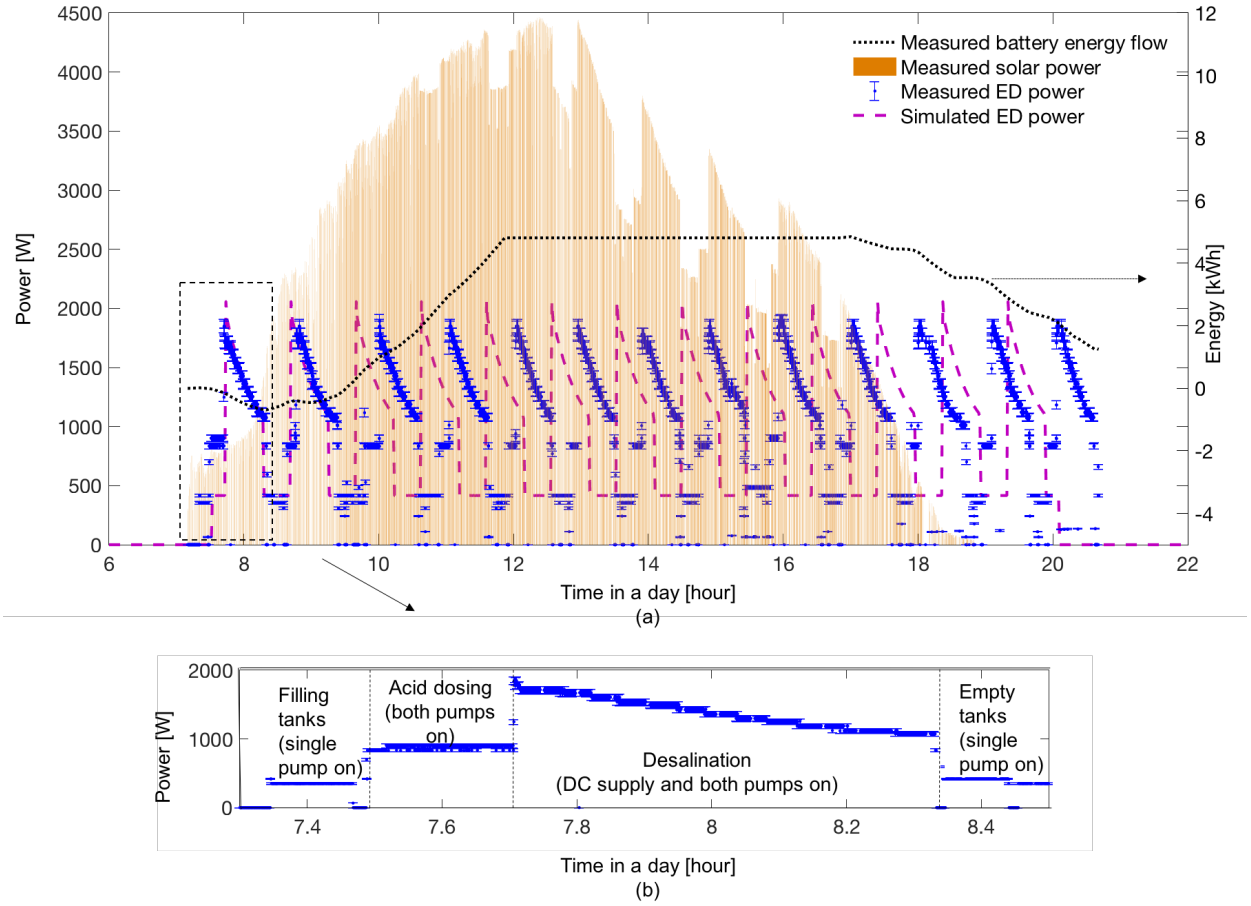

Figure 4: (a) Daily power profiles for the solar PV panels and ED system along with the energy flow of the batteries, from field testing of the Chelluru system on May 2, 2018. (b) A power profile of a single batch (shown by the dashed box in a) on the same day, including filling tanks, acid dosing, ED desalination in batch mode, and emptying tanks.

consumption of the RO plant is plotted along with the difference between production and consumption (which would be stored in the water tank) for the same day (May 2, 2018) in Fig. 6. This comparison shows how effective the PV-EDR system would be if it were supplying the daily drinking water needs of villagers in Chelluru. The results indicate that after the 13 batches, 5.9 m^3 of water was produced, with 2 m^3 stored in the water tank for future use. In Fig. 6, the negative values indicate that withdraw exceeds production. As we have chosen an empty tank (value 0) as the starting point, and the beginning of the day as our starting time, mathematically negative values appear. Although demand was not met in the morning on this particular day, as there was no water stored in the testing day, under normal operation over many days, there would be excess water stored in the tank from the previous day, which would be available in the morning. From the data shown in Fig. 6, that storage would be approximately 2 m^3, which is much larger than the deficit during the morning, indicating demand would likely be met throughout the entire day. During the design process, the actual water demand data for the village was not available; it was assumed to be constant, e.g. 6 m^3/day, throughout the year. If the water consumption is less than 6 m^3/day, more water will be stored in the tank for later use. This will typically be the condition of the system, as it was designed to meet 100% demand throughout the year.

Together, these results indicate: 1) the pilot PV-EDR system is capable of providing sufficient energy to produce the required volume of water on a

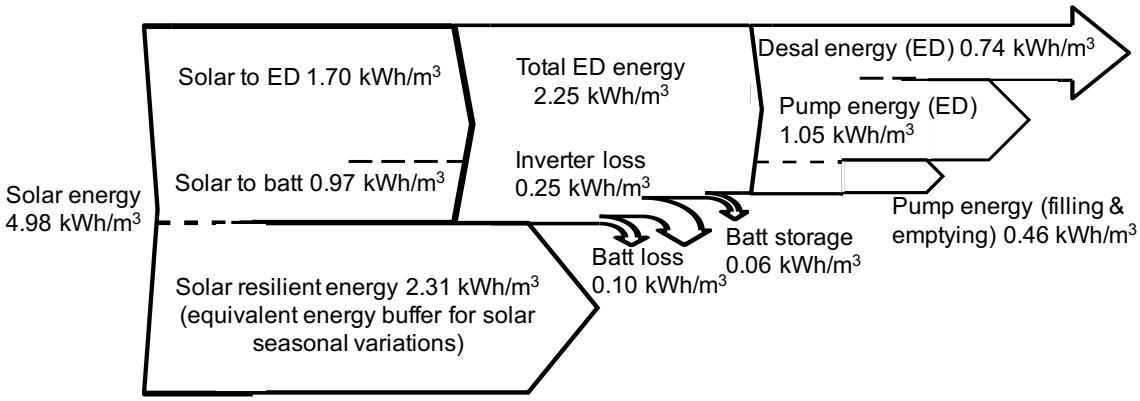

Figure 5: Sankey diagram of specific energy flow for field testing of the Chelluru system on May 2, 2018 showing daily energy flow. The uncertainty on SEC measurements is ± 7.5%.

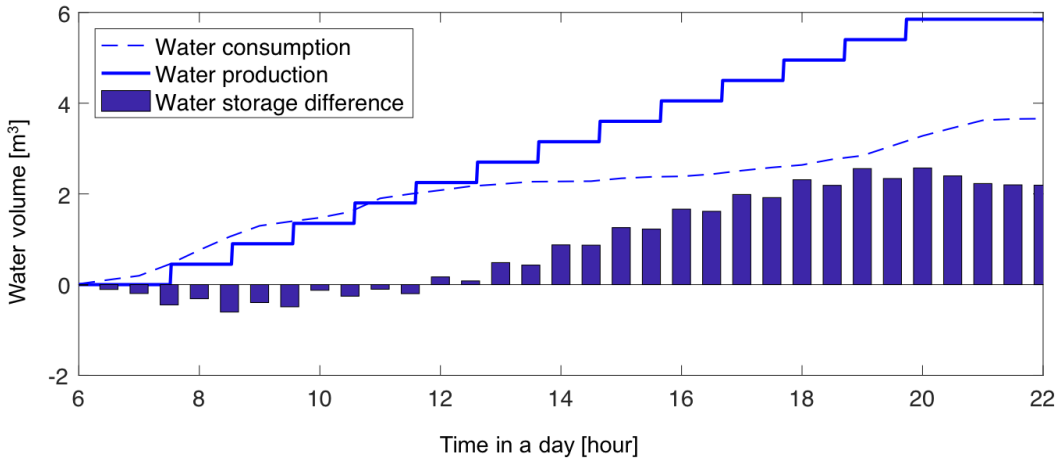

Figure 6: Daily production capability verses demand for water in Chelluru. The solid line denotes the cumulative water production of the PV-EDR desalination system over the course of the day on May 2, 2018. The dashed line is the cumulative water sold by the adjacent RO plant on the same day. The bar plot is the difference between the water production and the water consumption.

daily basis as expected; and 2) the holistic PV-EDR model is accurate in predicting water flow, and energy flow between the sub-systems. The daily multiple-batch ED power profile shows good agreement between simulation and experimental data. The daily energy flow of the battery demonstrates the capacity of the battery bank to charge, store, and discharge power sufficiently to complete the required number of ED batches over the day.

4.3. Long-term performance

An optimal PV-EDR system should not only provide sufficient water by utilizing the variable solar power from morning to night, but also have a capacity to deal with seasonal weather patterns and variations over a long period. To achieve this performance goal, the cost-optimal system design converged at a system that combined battery storage, water storage, and excess PV panels as energy buffers, allowing the system to overcome daily and

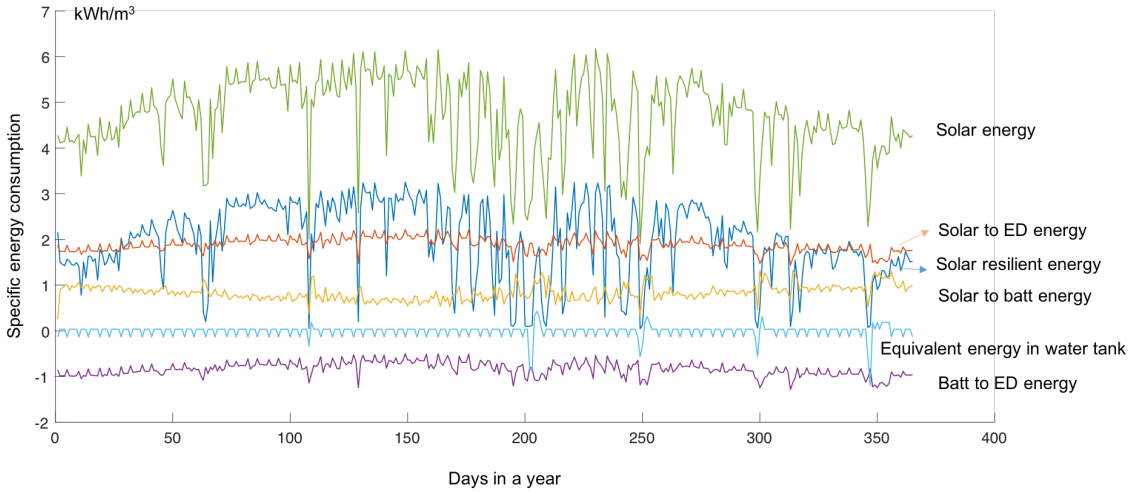

Figure 7: Simulated yearly energetic performance of the PV-EDR system over one year. The solar energy is broken into solar energy (total solar input), solar resilient energy, solar-to-ED energy (energy that directly powers the ED process), solar-to-battery energy (energy that charges the battery), equivalent energy in the water tank (energy stored in the water tank as desalinated water), and battery-to-ED energy (energy that the batteries discharge to power the ED process), plotted as SEC in kWh/m^3. These facets of how the system manages energy each have a different role to ensure water production with the lowest system cost.

seasonal variations in solar energy. The 46% of solar energy that was not being used by the pump or ED system on May 2 (analyzed in Section 3.3, Fig. 5) acts as solar resilient energy, which is an energy buffer equivalent to a battery or water storage that ensures system reliability during the worst solar conditions over the year. Other energy buffers, including battery and water storage, ensure system reliability over shorter timescales.

To demonstrate this effect, Fig. 7 shows the simulated yearly energetic performance of the pilot PV-EDR system, including solar energy (total solar input), solar resilient energy, solar-to-ED energy (energy that directly powers the ED process), solar-to-battery energy (energy that charges the battery), equivalent energy in the water tank (water stored in the water tank), and battery-to-ED energy (energy that the batteries discharge to power the ED process), plotted as SEC in kWh/m^3. The water volume (m^3) stored in the tank is converted to energy in kWh using the SEC of 2.25 kWh/m^3 as shown in Fig. 5. From Fig. 7, it is clear that the battery energy storage primarily manages the daily energy flow between the solar PV panels and the ED process, and is therefore primarily used as a buffer against daily solar variations. In contrast, the solar resilient energy closely follows the solar input energy, and approaches zero only to overcome the worst solar weather conditions during the year (e.g. around day 200 and day 250 in Fig. 7). This allows the solar resilient energy to provide energy to maintain the daily cycle of battery energy flow and water production. Water tank storage contributes primarily to maintain daily energy flow, and also provides water to meet the demand during the worst solar conditions of the year. Compared to large-scale pumped hydro storage [25, 26], water tanks have much lower CapEx for storing water. It is also much less expensive than batteries for storing energy for water production. The cost of water storage in tanks is 48 USD/kWh, only 33% of the cost of battery storage. Thus, the flexible water production and water storage is much suitable to small-scale desalination systems for minimizing the water cost. These insights can be used to understand the source of the trade-offs between long-term reliability and cost that result from changing the size of the different system components.

Trade-offs between long-term reliability and cost are further evident in the relatively low energy utilization rate from solar to the system, which was 54% on the measured day (Fig. 5) and only 61% over the year (Fig. 7). Demanding a high reliability over the worst seasonal conditions can be achieved by increasing panel size, water storage, battery storage, or water production capacity (i.e. ED stack

size). However, increasing battery storage and ED stack size (e.g. ED membrane area) are relatively expensive [15]. As a consequence, the most cost-effective way to achieve high reliability during the worst solar conditions is thus to increase PV panel area, which leads to oversizing the PV system for most of the year, creating a large amount of solar resilient energy. This was the case in the Chelluru system, indicated by the low utilization rates. This result is similar to the investigated renewable energy (solar or wind) powered desalination systems in the literature [25, 26, 27], which also achieve a low water cost while maintaining high reliability by oversizing the PV system for most of the year.

Therefore, to harness these large amounts of available but unused intermittent clean energy during much of the year, future innovations are needed to efficiently utilize this variable resilient solar energy. For example, flexible EDR operation that could vary its water production rate (and power consumption) to accommodate varying solar power at timescales of seconds, minutes, or hours, could significantly reduce the required battery capacity and better utilize the resilient solar energy. This would increase overall solar energy efficiency and could improve the energy flow between the PV, storage, and ED sub-systems, further reducing water cost.

5. Water cost analysis of the pilot PV-EDR system

The PV-EDR system capital cost and lifetime cost were re-evaluated using the validated and corrected PV-EDR holistic model that was used for the co-optimal system optimization (Section 4). Similar to [15], costs between the co-optimal design and a PV-EDR system designed through conventional design practice were compared. The same water production is targeted for both systems.

The system capital cost of major components, C_{sys}, is estimated by

$$C_{sys} = C_{PV}A_{PV} + C_{batt}E_{batt} + C_{tank}V_{tank} + C_{CP}N_{CP} + 2C_{elec} + 2C_{pump} + C_{inv}, \quad (11)$$

where C_{PV} is capital cost of the PV panels in USD/m^2, A_{PV} is the PV panel area, C_{batt} is the battery capital cost in USD/kWh, E_{batt} is the battery capacity, C_{tank} is the capital cost of the water tank in USD/m^3, V_{tank} is the volume of the tank, C_{CP} is the membrane capital cost in USD/pair, N_{CP} is the number of membrane pairs, C_{elec} is the capital cost per electrode, C_{pump} is the capital cost per pump, and C_{inv} is capital cost per inverter. The cost of accessories such as valves and pipes are expected to be relatively small compared to other costs and are thus not considered here.

To estimate the lifetime cost of the system, a levelized cost of water (LCOW) model which is similar to that used in [34] was utilized,

$$LCOW = \frac{crfC_{sys} + C_{O,M,R}}{V_{water}^{year}}, \quad (12)$$

$$crf = \frac{k_d(1+k_d)^n}{(1+k_d)^n - 1}, \quad (13)$$

where k_d is annual interest rate, n is depreciation period in years, $C_{O,M,R}$ is total annual cost for operation, maintenance, and replacement, and V_{water}^{year} is annual water produced for the village.

The cost parameters used in the economic analysis are listed in Table 4. A depreciation period of 20 years and an interest rate of 8% was used. The lifetime of the pumps and lead-acid batteries was assumed to be 5 years [7, 15] with converted annual replacement costs of USD96 and USD30, respectively. The PV panels and membrane were assumed to have 20-year and 10-year lifetimes respectively [15], and the resulting costs are listed in Table 4.

It should be noted that the cost estimation above under-estimates the system cost and water cost, because it only considers the cost of major components, as listed in Table 4. However, this estimation is a reasonable metric of comparison between the optimized PV-EDR system and one designed using conventional design practice, as it captures the major cost drivers. Fig. 8 shows the cost breakdown of the Chelluru system versus the cost of the system designed following a conventional, sequential design practice, which is described in Appendix A.

It is important to note that the Chelluru system is a prototype and has not yet had the benefits of other commercially available technologies, such as economies of scale. Therefore, while capital cost and LCOW estimates are useful to compare conventionally designed PV-EDR systems to the Chelluru system, these costs should not be taken as representative of the expected PV-EDR costs at scale. The capital cost (Fig. 8a) of the co-optimal design including all major components as considered in Equation 11 is USD21,498, which is 34% lower than the capital cost of the conventionally designed

Table 4: Capital, operational, maintenance, and replacement costs used in the cost analysis.

Parameters	**Value**
PV panel [USD/m^2]	98 [6]
Batteries [USD/kWh]	150 [6]
Water tank [USD/m^3]	110 [6]
ED membranes [USD/pair]	150 [6]
Electrode [USD]	2,000 [6]
Pump [USD]	239 [6]
Inverter [USD]	1,200 [35]
Pump replacement [USD/year]	96 [15]
PV operation & maintenance [USD/m^2/year]	5 [7]
Battery replacement [USD/kWh/year]	30 [15]
Membrane maintenance & replacement [USD/pair/year]	20 [7, 15]

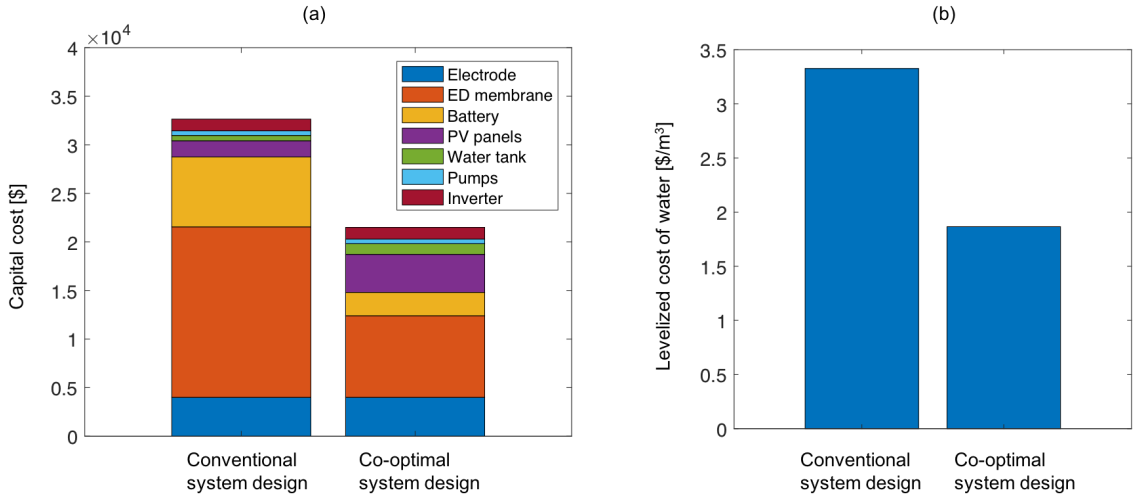

Figure 8: Analysis of the capital cost of the PV-EDR pilot system designed using the optimization theory presented herein versus conventional design practice in terms of (a) capital cost of the components that are primary cost drivers, and (b) levelized cost of water.

system at USD32,644. This reduction was achieved by utilizing fewer membranes, fewer batteries, and "over-sized" PV panels as discussed in Section 4. The LCOW (Fig. 4b) as described by Equation 12 and Equation 13 is also significantly lower for the co-optimal design, at 1.87 USD/m^3 compared to 3.33 USD/m^3 for the conventional system - a 45% savings. This relatively large cost reduction is primarily due to the reduced lifetime cost of batteries in the co-optimal designed Chelluru system. Both the capital cost and the LCOW show substantial cost reductions, demonstrating the effectiveness of the co-optimization framework for community-scale PV-EDR systems using off-the-shelf components to provide water in rural India. In addition, the on-grid RO desalination system located in Chelluru is sustainably maintained by selling drinking water at ₹2-3 per 12 L (2.4-3.6 USD/m^3) [7]. Even without the benefit of economies of scale, the estimated LCOW indicates that this PV-EDR system has the potential to maintain a profitable water business in rural India.

The conventionally designed PV-EDR system and co-optimal PV-EDR system can be compared using metrics other than cost, depending on the priorities of the user. For example, comparing the system designs of Table 1 and Table 5, the co-optimal system requires less indoor space to install because it has a smaller ED stack and fewer batteries. However, it may require more outdoor space due to more tank storage and larger solar panel area. Compared to solar panels, batteries require more monitoring

and maintenance (such as temperature control) to avoid rapid degradation. The co-optimal system design, with reduced battery capacity and larger water tank storage, might be favorable in this case, particularly in hot climates. The different designs will also have different environmental and net energy impacts [36], though a full life cycle analysis or environmental impact assessment is beyond the scope of the current study.

6. Conclusions

This study presents experimental tests of a community-scale, co-optimized PV-EDR pilot system operated in the rural village of Chelluru, India. These field tests allowed for an improved understanding, and correction, of the behavior of our previous presented PV-EDR design theory [15] based on real-world factors. Time consumed for filling and draining tanks in the Chelluru system was unaccounted in the initial simulation, limiting operating time and daily production rate of the system. Salt and water not flushed out after a prior batch created different starting concentrations of the diluate and concentrate flows, which noticeably changed the performance of the desalination process. Energy losses due to lower than expected efficiencies, especially of the DC supply, were indicative of local constraints that would have been difficult to predict before testing. Scaling was a significant issue in Chelluru and led to implementing procedures for acid rinsing and dosing, as well as running the system at a lower recovery ratio than originally intended. Addition of these real-world factors to the proposed PV-EDR model allowed for accurate prediction of the performance of the pilot system. Hopefully these lessons will educate other desalination system designers and help them avoid similar unanticipated, real-world particularities.

In the field test, the PV-EDR pilot successfully desalinated real groundwater in Chelluru to the required quality (TDS $\leq$ 300 mg/L) in a sufficient quantity. The holistic PV-EDR model is predictive of ED system performance (e.g. concentration, current, and power), and of the power/energy flow between the PV panels, battery, and ED stack with high accuracy. This holistic model was used as the foundation for the co-optimal design theory, which enabled the exploration of system designs with the least cost and satisfactory performance. The pilot PV-EDR system in Chelluru indicated the co-optimal design theory presented in [15] effectively balanced the system cost-performance trade-offs, and managed both short-term and long-term solar intermittence and variance by leveraging PV panel area, battery storage, and desalinated water storage as energy buffers. Therefore, the design theory with the holistic model provides a useful tool for off-grid ED designers to minimize water cost while maintaining desired system performance and reliability, and accounting for local factors.

By comparing the cost estimated using the major components in the pilot system, the co-optimal Chelluru system achieved 34% and 45% saving in the estimated capital cost and LCOW, respectively, compared to the costs of an equivalently sized PV-EDR system designed using conventional design practice. These cost reductions demonstrate the effectiveness of the co-optimal design theory as a cost-reduction method. Though some factors (e.g. elements of the ED stack cost beyond electrodes and membranes) are not included, the estimated LCOW (1.87 USD/m^3) is much lower than the current water selling price of water produced with RO in Indian villages (2.4-3.6 USD/m^3).

These results indicate that PV-EDR could become a commercially viable solution in rural Indian communities. To this aim, future technical efforts will focus on addressing factors that will reduce the cost of PV-EDR systems and improve their reliability, such as fully optimizing the ED stack (membrane and electrode area, and number of cell pairs); mitigating scale formation; improving recovery; reducing system footprint; and utilizing improved power management components with better efficiency. The mechanical design of a future community-scale ED stack could also be optimized for a reduced size, which could substantially reduce the cost of community-scale PV-EDR systems in rural India. The analysis in this study was carried out using an off-the-shelf ED stack designed for commercial, large-scale desalination plants. In future iterations, membrane and electrode area could be adjusted as parameters, resulting in optimal designs with smaller ED stacks, significantly reducing the cost. ED stack size could also be reduced with improved flexible operation to more effectively utilize variable solar power supply. A highly flexible EDR system could adaptively vary its water production rate on timescales of seconds, minutes, or hours, enabling the energy consumption of EDR to closely follow the variable solar power supply. This could significantly reduce the required battery capacity for water production, further reducing water

costs.

7. Acknowledgments

This work was sponsored by Tata Projects Ltd., the United States Bureau of Reclamation Desalination and Water Purification Research and Development Grants R16AC00122 and R17AC00150, and the MIT Energy Initiative. I.M.P and T.B acknowledge the support from Singapores National Research Foundation through the Singapore MIT Alliance for Research and Technology's 'Low energy electronic systems (LEES) IRG'.

References

[1] N. Aayog, Composite water management index (2018).

[2] M. M. Mekonnen, A. Y. Hoekstra, Four billion people facing severe water scarcity, Science advances 2 (2) (2016) e1500323.

[3] S. India, Ground water quality in shallow aquifer of india, Available at `https://www.indiastat.com/table/villages/6376/ruralfacilities/281388/281420/data.aspx` (2018/08/23).

[4] Bureau of indian standards, drinking water - speci cation (second revision is 10500) (2012).

[5] Indiastat, Available at `https://www.indiastat.com/table/villages/6376/ruralfacilities/281388/281420/data.aspx` (2018/08/23).

[6] David, Development, and field-testing of a cost-optimized village-scale, photovoltaic-powered, electrodialysis reversal water desalination system for rural india (June 2018).

[7] M. SreeRame, Personal conversation (Sptember 2017).

[8] N. C. Wright, et al., Justification for community-scale photovoltaic-powered electrodialysis desalination systems for inland rural villages in india, Desalination 352 (2014) 82–91.

[9] S. G. Banerjee, D. Barnes, B. Singh, K. Mayer, H. Samad, Power for all: Electricity access challenge in India, The World Bank, 2014.

[10] S. Manju, N. Sagar, Renewable energy integrated desalination: A sustainable solution to overcome future fresh-water scarcity in india, Renewable and Sustainable Energy Reviews 73 (2017) 594–609.

[11] J. Ortiz, E. Expósito, F. Gallud, V. García-García, V. Montiel, A. Aldaz, Photovoltaic electrodialysis system for brackish water desalination: Modeling of global process, Journal of Membrane Science 274 (1-2) (2006) 138–149.

[12] A. Gonzalez, M. Grágeda, S. Ushak, Assessment of pilot-scale water purification module with electrodialysis technology and solar energy, Applied Energy 206 (2017) 1643–1652.

[13] M. R. Adiga, S. Adhikary, P. Narayanan, W. Harkare, S. Gomkale, K. Govindan, Performance analysis of photovoltaic electrodialysis desalination plant at tanote in thar desert, Desalination 67 (1987) 59–66.

[14] O. Kuroda, S. Takahashi, S. Kubota, K. Kikuchi, Y. Eguchi, Y. Ikenaga, N. Sohma, K. Nishinoiri, S. Wakamatsu, S. Itoh, An electrodialysis sea water desalination system powered by photovoltaic cells, Desalination 67 (1987) 33–41.

[15] D. W. Bian, S. M. Watson, N. C. Wright, S. R. Shah, T. Buonassisi, D. Ramanujan, I. M. Peters, et al., Optimization and design of a low-cost, village-scale, photovoltaic-powered, electrodialysis reversal desalination system for rural india, Desalination 452 (2019) 265–278.

[16] P. Tsiakis, L. G. Papageorgiou, Optimal design of an electrodialysis brackish water desalination plant, Desalination 173 (2) (2005) 173–186.

[17] H. Laborde, K. Franca, H. Neff, A. Lima, Optimization strategy for a small-scale reverse osmosis water desalination system based on solar energy, Desalination 133 (1) (2001) 1–12.

[18] A. M. Bilton, L. C. Kelley, Design of power systems for reverse osmosis desalination in remote communities, Desalination and Water Treatment 55 (10) (2015) 2868–2883.

[19] F. Vince, F. Marechal, E. Aoustin, P. Bréant, Multi-objective optimization of ro desalination plants, Desalination 222 (1-3) (2008) 96–118.

[20] A. M. Bilton, R. Wiesman, A. Arif, S. M. Zubair, S. Dubowsky, On the feasibility of community-scale photovoltaic-powered reverse osmosis desalination systems for remote locations, Renewable Energy 36 (12) (2011) 3246–3256.

[21] T. N. Bitaw, K. Park, D. R. Yang, Optimization on a new hybrid forward osmosis-electrodialysis-reverse osmosis seawater desalination process, Desalination 398 (2016) 265–281.

[22] W. He, Y. Wang, M. H. Shaheed, Stand-alone seawater ro (reverse osmosis) desalination powered by pv (photovoltaic) and pro (pressure retarded osmosis), Energy 86 (2015) 423–435.

[23] W. Peng, A. Maleki, M. A. Rosen, P. Azarikhah, Optimization of a hybrid system for solar-wind-based water desalination by reverse osmosis: Comparison of approaches, Desalination 442 (2018) 16–31.

[24] S. Kumarasamy, S. Narasimhan, S. Narasimhan, Optimal operation of battery-less solar powered reverse osmosis plant for desalination, Desalination 375 (2015) 89–99.

[25] C. R. Henderson, J. F. Manwell, J. G. McGowan, A wind/diesel hybrid system with desalination for star island, nh: feasibility study results, Desalination 237 (1-3) (2009) 318–329.

[26] I. D. Spyrou, J. S. Anagnostopoulos, Design study of a stand-alone desalination system powered by renewable energy sources and a pumped storage unit, Desalination 257 (1-3) (2010) 137–149.

[27] Y. Zhang, L. Pinoy, B. Meesschaert, B. Van der Bruggen, A natural driven membrane process for brackish and wastewater treatment: photovoltaic powered ed and fo hybrid system, Environmental science & technology 47 (18) (2013) 10548–10555.

[28] S. Watson, D. Bian, N. Sahraei, A. G. Winter, T. Buonassisi, I. M. Peters, Advantages of operation flexibility and load sizing for pv-powered system design, Solar Energy 162 (2018) 132–139.

[29] N. C. Wright, S. R. Shah, S. E. Amrose, A. G. Winter, A robust model of brackish water electrodialysis desalination with experimental comparison at different size scales, Desalination 443 (2018) 27–43.

[30] National solar radiation data base, Available at http://rredc.nrel.gov/solar/old_data/nsrdb/ (2018/08/23).
[31] F. Edition, Guidelines for drinking-water quality, WHO chronicle 38 (4) (2011) 104–8.
[32] SUES fact sheet, ionics* ion exchange membrane, Available at https://my.suezwatertechnologies.com/ (2019/10/02).
[33] W. E. Katz, The electrodialysis reversal (edr) process, Desalination 28 (1) (1979) 31–40.
[34] J. Lienhard, M. A. Antar, A. Bilton, J. Blanco, G. Zaragoza, Solar desalination, Annual review of heat transfer 15 (15).
[35] Amazon, Available at https://www.amazon.in/UTL-SOLAR-PCU-7-5-VOLTS/dp/B076SM5XM5 (2018/08/23).
[36] D. Ramanujan, N. Wright, S. Truffaut, G. von Medeazza, A. Winter, Sustainability analysis of pv-powered electrodialysis desalination for safe drinking water in the gaza strip, in: Proceedings of the IDA 2017 World Congress on Water Reuse and Desalination, São Paulo, Brazil, 2017, pp. 15–20.

8. Appendix

8.1. Appendix A: the conventional sequential design method

This section describes the design of a PV-EDR system using a conventional, sequential design practice as a point of comparison to the co-optimal design presented in the main body of the paper. This rule-of-thumb design is based on the design method presented in [15]. First, two design criteria were applied: 1) a daily water production requirement for the Chelluru village of 6 m^3, and 2) a daily operation period of 8 hours per day, which is the current operation period of the on-grid RO system installed in Chelluru. This resulted in a nominal flow rate of 750 liter per hour (LPH). Second, the ED unit was optimally designed according to the production rate and local groundwater quality. The water recovery ratio was set to 60%, which is same as the co-optimal system. The batch size was set to 1 m^3 because it corresponds to the most common tank size available locally. Based on these criteria, the optimal ED unit had 117 membrane pairs and an applied voltage of 78 V. Pumps were selected based on the inventory of Tata Projects Ltd., which assumed the same costs as the co-optimal design. The resulting daily energy consumption of the conventional EDR system was approximately 12 kWh to run 6 batches per day. For electrical energy storage, a battery capable of supplying two days of back-up was recommended, resulting in 48 kWh of battery storage, assuming 50% as the minimum depth of charge.

India's average daily global horizontal irradiance solar resource for the region is approximately 6 kWh/m^2/day. Thus, the required PV panels for powering the system was estimated by

$$A_{PV} = f\frac{E_{EDR,d}}{\eta_{PV}E_{PV,d}}, \tag{14}$$

where f is the scaling coefficient which accounts for losses, η_{PV} is efficiency of the solar panels, $E_{PV,d}$ is the daily energy consumption by ED, and $E_{PV,d}$ is the daily energy generation by unit area of PV. If the scaling coefficient f is 1.3, the required solar PV panel area is about 17 m^2. For water storage, a 5 m^3 water tank was selected.

The system parameters for the resulting conventional design of a PV-EDR system are given in Table 5, with the associated capital costs listed in Table 4.

Table 5: The rule-of-thumb design of the PV-EDR system in Chelluru.

Design variables	**Value**
PV area m^2	17
Battery capacity kWh	48
Water storage volume m^3	5
ED cell pairs	117
Batch size m^3	1
Electrodes	2
Pump	2

8.2. Appendix B: compositions of groundwater in Chelluru

The composition of feed water in Chelluru was reported in [29] and is repeated in Table 6. The final column shows the molar mass to charge ratio (M/z) for each constituent, where the ratio for CO_3^{2-} is shown in the alkalinity row. The feed water in Chelluru was particularly high in calcium with a pH of 7.02±0.12. These conditions made the Chelluru site particularly susceptible to scaling.

Table 6: The major constituents in the feed water in Chelluru [29]

Parameters	**Value**
Sodium as Na, mg/L	142±25
Magnesium as Mg, mg/L	66.8±6.3
Calcium as Ca, mg/L	230±22
Potassium as K, mg/L	20±1.8
Chlorides as Cl, mg/L	382±37
Sulphates as SO_4, mg/L	72.4±6.6
Nitrates as NO_3, mg/L	43.1±3.9
Alkalinity HCO_3 as $CaCO_3$, mg/L	648±56
Total dissolved solids TDS, mg/L	1490±103
Electrical conductivity at 25 °C, μS/cm	2480±55
Turbidity, NTU	0.6
Iron as Fe, mg/L	0.01±0.001
Sulphide as H_2S, mg/L	<0.01
Silica as SiO_2, mg/L	<1.0
Boron as B, mg/L	<0.01
pH at 25 °C	6.9±0.7